2.5 Geology, Seismology, and Geotechnical Engineering

NAPS COL 2.0-26-A
NAPS COL 2.0-27-A
NAPS COL 2.0-28-A
NAPS COL 2.0-29-A
NAPS COL 2.0-30-A

The information needed to address DCD COL Items 2.0-26-A, 2.0-27-A, 2.0-28-A, 2.0-29-A, and 2.0-30-A are included in SSAR Section 2.5, which is incorporated by reference with the following variance and supplements. Vertical datum is with reference to NAVD88 throughout Section 2.5, unless stated otherwise.

The first two paragraphs of SSAR Section 2.5 are replaced as follows.

NAPS ESP VAR 2.0-4

This section presents information on the geological, seismological, and geotechnical engineering properties of the Unit 3 site and the region surrounding the site. Section 2.5.1 describes basic geological and seismologic data based on those data developed since publication of the EPRI 1986 seismic source model (SSAR Reference 1) with additional information based on the Central and Eastern United States Seismic Source Characterization (CEUS SSC) for Nuclear Facilities Project (Reference 2.5-223) and the moment magnitude (**M**) 5.8 earthquake that occurred near Mineral, Louisa County, VA on August 23, 2011. Section 2.5.2 describes the vibratory ground motion at the site, the CEUS SSC model as documented in NUREG-2115 (Reference 2.5-223), and an update of the seismicity catalog. The CEUS SSC model, which incorporates the Electric Power Research Institute (EPRI) ground motion prediction equations (GMPEs) (References 2.5-224 and 2.5-225), is used to perform a hard rock probabilistic seismic hazard analysis (PSHA) and develop uniform hazard response spectra (UHRS). Site-specific strong ground motion amplification factors are developed using properties of subsurface materials described in Section 2.5.4. These amplification factors and the hard rock UHRS are combined to define the ground motion response spectra (GMRS) following the guidance in RG 1.208, A Performance-Based Approach to Define the Site-Specific Earthquake Ground Motion (Reference 2.5-226). Section 2.5.3 describes the potential for surface faulting in the site area, and Sections 2.5.4, 2.5.5, and 2.5.6 describe the stability of surface materials and foundations at the site.

RG 1.208, Appendix C, “Investigations to Characterize Site Geology, Seismology and Geophysics” (Reference 2.5-226), provides guidance for the level of investigation recommended at different distances from a proposed site for a nuclear facility. The site region is that area within

200 miles (320 km) of the site location. The site vicinity is that area within 25 miles (40 km) of the site location. The site area is that area within 5 miles (8 km) of the site location. The site is that area within 0.6 mile (1 km) of the site location. These terms, site region, site vicinity, site area, and site, are used in Sections 2.5.1 through 2.5.3 to describe these specific areas of investigation. These terms are not applicable to other sections of the FSAR.

2.5.1 Basic Geologic and Seismic Information

NAPS COL 2.0-26-A

The information needed to address DCD COL Item 2.0-26-A is included in SSAR Section 2.5.1, which is incorporated by reference with the following variance and supplements.

The first three paragraphs of SSAR Section 2.5.1 are replaced as follows.

NAPS ESP VAR 2.0-4

This section presents information on the geological and seismological characteristics of the Unit 3 site region and area. The information is divided into two parts. SSAR Section 2.5.1.1 describes the geologic and tectonic setting of the site region and SSAR Section 2.5.1.2 describes the geology and structural geology of the site area. The geological and seismological information was developed in accordance with the guidance presented in RG 1.70, Section 2.5.1, “Basic Geologic and Seismic Information” (SSAR Reference 3), RG 1.206, “Combined License Applications for Nuclear Power Plants” (Reference 2.5-203), and RG 1.208. This information is intended to satisfy the requirements of 10 CFR 100, “Reactor Site Criteria,” Section 100.23, “Geologic and Seismic Siting Criteria,” paragraph (c) “Geological, Seismological and Engineering Characteristics” (SSAR Reference 4). The geological and seismological information presented in this section are used as a basis for evaluating the geologic, seismic, and man-made hazards at the site.

RG 1.208 states that seismic sources identified and characterized by EPRI (References 2.5-227 and 2.5-228) and Lawrence Livermore National Laboratory (LLNL) (References 2.5-229, 2.5-230, and 2.5-231) are to be used for studies in the CEUS. However, the EPRI-SOG model and the LLNL model were replaced by the CEUS SSC model and database (Reference 2.5-223).

The geological and seismological information presented in this section was developed from a review of previous reports prepared for existing

Units 1 and 2 and the abandoned Units 3 and 4, published geologic literature, interpretation of aerial photography, subsurface investigations, and field and aerial reconnaissance. Previous site-specific reports reviewed include the existing Units 1 and 2 UFSAR (SSAR Reference 5) and ISFSI Safety Analysis Report (SSAR Reference 6). Reports prepared by Dames and Moore for design and construction of the existing units (SSAR Reference 7) and the abandoned Units 3 and 4 (SSAR References 8 and 9) were also reviewed. A review of published geologic literature was used to supplement and update the existing geological and seismological information. This literature was identified using the GeoRef database (American Geological Institute) and the USGS library catalogue. In addition, relevant unpublished geologic literature, studies, and projects were identified by contacting the USGS, State geological survey organizations, and universities. This section includes information on the **M** 5.8 earthquake that occurred on August 23, 2011 in Mineral, Louisa County, Virginia, and the results of a geological reconnaissance to investigate any surface features associated with the earthquake in the site vicinity. A list of the references used to compile the geological and seismological information presented in the following sections is provided at the end of Section 2.5.

2.5.1.1.4 Regional Tectonic Setting

The first two paragraphs of SSAR Section 2.5.1.1.4 are replaced as follows.

NAPS ESP VAR 2.0-4

The CEUS SSC Project was conducted by EPRI, the DOE, and the NRC from April 2008 to December 2011. The purpose of this project was to provide a regional seismic source model for use in the PSHA for a nuclear facility in the CEUS. This study replaces regional seismic source models developed for performing a PSHA including the EPRI-SOG model and the LLNL model. The CEUS SSC model is described in detail in Reference 2.5-223.

The following four sections (a-d) describe the site region in terms of plate tectonic evolution, origin and orientation of tectonic stress, primary tectonic features, and previously-defined seismic sources. Figure 2.5.1-202 provides an overview of the eastern United States and the seismotectonic zones from the CEUS SSC. The CEUS SSC host source for the Unit 3 site is the Extended Continental Crust-Atlantic

Margin Zone (ECC-AM) defined to include the region characterized by the presence of extended continental crust developed during Mesozoic rifting along the Atlantic Ocean basin margin (Reference 2.5-223). The ECC-AM and the source immediately to the west, the Paleozoic Extended Crust Zone (PEZ) are characterized by the geologic structures described below. The Atlantic Highly Extended Crust Zone (AHEX) is located to the east of the ECC-AM and represents the region of highly extended crust that is the transition between the extended, thick continental crust of the ECC-AM and the thinner mafic oceanic crust (Atlantic Ocean basin). Historical seismicity occurring in the site region is described in Section 2.5.2.1. The CEUS SSC methodology and seismic sources relevant to the Unit 3 site are described in greater detail in Sections 2.5.2.2.3 and 2.5.2.3.

a. **Plate Tectonic Evolution of the Appalachian Orogenic Belt at the Latitude of the Site Region**

The first sentence of the third paragraph of Item a of this SSAR section is replaced as follows.

NAPS ESP VAR 2.0-4

SSAR Figure 2.5-6 is a simplified tectonic map showing the five onshore physiographic provinces of Virginia and the belts and terranes within the Blue Ridge and Piedmont Provinces, as delineated by Hatcher (SSAR Reference 45) and Horton and others (SSAR Reference 46).

The second sentence of the eighth paragraph of Item a of this SSAR section is replaced as follows.

NAPS ESP VAR 2.0-4

This model represents a significant alternative interpretation of the origin and affinity of the crust east of the Spotsylvania thrust fault in the region of the Unit 3 site.

b. **Tectonic Stress in the Mid-Continent Region**

NAPS ESP VAR 2.0-4

The last paragraph of Item b of this SSAR section is deleted.

c. Principal Tectonic Structures

1. Paleozoic Tectonic Structures

The last sentence of the third paragraph of Item 1 under Item c of this SSAR section is replaced as follows.

NAPS ESP VAR 2.0-4

Therefore, these Paleozoic structures in the site region are not considered to be capable tectonic sources, as defined in RG 1.208, Appendix A.

The last sentence of the fourth paragraph of Item 1 under Item c of this SSAR section is replaced as follows.

NAPS ESP VAR 2.0-4

None of the faults located within 25 miles of the site are considered to be capable tectonic sources, as defined in RG 1.208, Appendix A.

NAPS ESP VAR 2.0-4

The last paragraph of Item 1 under Item c of this SSAR section is deleted.

2. Mesozoic Tectonic Structures

The first sentence of the first paragraph of Item 2 under Item c of this SSAR section is replaced as follows.

NAPS ESP VAR 2.0-4

Mesozoic basins have long been considered potential sources for earthquakes along the eastern seaboard and are considered to be characteristic of the ECC-AM Zone which is described in the CEUS SSC (Reference 2.5-223).

The first sentence of the second paragraph of Item 2 under Item c of this SSAR section is corrected as follows.

NAPS COR

Generally, the exposed rift basins are asymmetric half-grabens (SSAR Figure 2.5-9) with the primary rift-bounding faults on the western margin of the half-grabens.

The last paragraph of Item 2 under Item c of this SSAR section is replaced as follows.

NAPS ESP VAR 2.0-4

Crone and Wheeler (SSAR Reference 59) do not recognize any basin-margin faults that have been reactivated during the Quaternary in the site region. No Mesozoic basin in the site region is associated with a known capable tectonic source. Seismicity potentially associated with

reactivation of faults bordering or beneath the Mesozoic basins is addressed in the CEUS SSC model (Reference 2.5-223).

3. **Tertiary Tectonic Structures**

The last paragraph under **Stafford Fault System** of Item 3 under Item c of this SSAR section is replaced as follows.

NAPS ESP VAR 2.0-4

The Stafford fault system is located within the ECC-AM (Reference 2.5-223). Field and aerial reconnaissance did not reveal any geologic or geomorphic features indicative of potential Quaternary activity along the fault system. Similarly, Crone and Wheeler (SSAR Reference 59) do not show the Stafford fault system as a Quaternary structure in their compilation of active tectonic features in the CEUS. The Stafford fault system, therefore, is not a capable tectonic source.

4. **Quaternary Tectonic Features**

A paragraph is added to the end of Item 4 under Item c of this SSAR section as follows.

NAPS ESP VAR 2.0-4

Aftershock data associated with the August 23, 2011, **M** 5.8 Mineral earthquake have been interpreted as a previously unmapped geologic structure, which Horton et al. (Reference 2.5-223) has termed the “Quail fault.” The “Quail fault” is a seismogenic structure (described in Section 2.5.1.1.7). Information on the Mineral earthquake is provided in Section 2.5.2. This structure does not fit the criteria for a repeated large-magnitude earthquake (RLME) source as defined in Reference 2.5-223. See Section 2.5.2.2.5.1.

The last two sentences of the second paragraph under **Paleo-Liquefaction Features within the Central Virginia Seismic Zone** of Item 4 under Item c of this SSAR section are replaced as follows.

NAPS ESP VAR 2.0-4

These paleo-liquefaction features do not fit the criteria for RLME sources and are considered within the ECC-AM source zone in the CEUS SSC model (Reference 2.5-223).

The last sentence of the sixth paragraph under **Mountain Run Fault Zone** of Item 4 under Item c of this SSAR section is replaced as follows.

NAPS ESP VAR 2.0-4

It is concluded that the Mountain Run fault zone is not a capable tectonic source. The Evarona-Mountain Run fault zone is not defined as an RLME source and is considered within the ECC-AM seismic source zone in the CEUS SSC model (Reference 2.5-223).

NAPS ESP VAR 2.0-4

The last sentence of the second paragraph and the third paragraph under **East Coast Fault System** of Item 4 under Item c of this SSAR section are deleted.

The first and second sentences of the fourth paragraph under **East Coast Fault System** of Item 4 under Item c of this SSAR section are replaced as follows.

NAPS ESP VAR 2.0-4

The southern segment of the East Coast Fault System (ECFS) is in essence covered by the different Charleston source zone geometries.

NAPS ESP VAR 2.0-4

The fourth and fifth sentences of the fifth paragraph under **East Coast Fault System** of Item 4 under Item c of this SSAR section are deleted.

The third and fourth sentences of the sixth paragraph under **East Coast Fault System** of Item 4 under Item c of this SSAR section are replaced as follows.

NAPS ESP VAR 2.0-4

Geomorphic analyses and aerial reconnaissance indicate that the northern segment of the fault zone probably does not exist or has a very low probability of activity if it does exist. The ECFS is not defined as an RLME source and is considered within the ECC-AM seismic source zone in the CEUS SSC model (Reference 2.5-223).

d. **Seismic Sources Defined by Regional Seismicity**

The first sentence of the first paragraph of Item d of this SSAR section is replaced as follows.

NAPS ESP VAR 2.0-4

Within 200 miles of the Unit 3 site, two previously recognized seismic sources are defined by a concentration of small to moderate earthquakes.

1. **Central Virginia Seismic Zone**

The fourth paragraph of Item 1 under Item d of this SSAR section is replaced as follows.

NAPS ESP VAR 2.0-4

Upper-bound maximum values of M_{max} used by the EPRI teams range from m_b 6.6 to 7.2 (SSAR Reference 1). Bollinger (SSAR Reference 79) estimated an M_{max} of m_b 6.4 for the Central Virginia seismic source. Chapman and Krimgold (SSAR Reference 57) have used an M_{max} of m_b 7.25 for the Central Virginia seismic source and most other sources in their seismic hazard analysis of Virginia.

However, new data and information on seismicity and seismic sources in the CEUS have led to the development of the CEUS SSC model. The Central Virginia Seismic Zone (CVSZ) is located within and comprises a portion of the ECC-AM Zone as defined by the CEUS SSC Project (Reference 2.5-223).

The August 23, 2011 earthquake has been referred to as both the Mineral, Virginia earthquake (References 2.5-233 and 2.5-234) and the Louisa County, Virginia earthquake (Reference 2.5-235). In the descriptions that follow, the term Mineral earthquake is used. The magnitude of the mainshock has been reported as both **M** 5.8 (References 2.5-233, 2.5-236, 2.5-237, 2.5-238, 2.5-239, and 2.5-240) and **M** 5.7 (References 2.5-234 and 2.5-241). The updated seismicity catalog in Section 2.5.2.1 designates the Mineral earthquake as **M** 5.8. The Mineral earthquake resulted from reverse faulting at a relatively shallow depth, approximately 4.7 mi (7.5 km), in central Virginia (Figure 2.5.1-201) (References 2.5-232, 2.5-235, and 2.5-237). More recent analyses indicate that the main shock hypocenter originated at 6.0 ± 3.1 km depth (Reference 2.5-268). Additional information on the Mineral earthquake is presented in Sections 2.5.2.1.3 and 2.5.2.2.5.1. Seismicity in this region is attributed to the CVSZ, as described above.

In order to best represent the approximate rupture plane or fault that produced the Mineral earthquake, the aftershock information provided on the Virginia Tech Seismological Observatory (VTSO) website (Reference 2.5-242), and described in Section 2.5.1.1.7, was used to develop a representation of the possible rupture plane and its up-dip projection to the surface (Figure 2.5.1-203). These seismologic data, analyses, and the results of a geological reconnaissance indicate that

there is no evidence of surface rupture or deformation of the ground surface. See Sections 2.5.1.1.7 and 2.5.2.3 for further descriptions of this topic. Several liquefaction features were generated by the Mineral earthquake and are described by researchers who investigated the epicentral area immediately following the earthquake (References 2.5-233 and 2.5-243).

2. **Giles County Seismic Zone**

The fourth paragraph of Item 2 under Item d of this SSAR section is replaced as follows.

NAPS ESP VAR 2.0-4

The largest known earthquake to occur in this region is the 1897 **M** 5.9 Giles County event (Section 2.5.2.1.3). Bollinger (SSAR Reference 79) estimated an M_{max} of m_b 6.3 for the Giles County seismic source using three different methods. Chapman and Krimgold (SSAR Reference 57) used an M_{max} of m_b 7.25 for the Giles County zone and most other sources in their seismic hazard analysis of Virginia. These estimates of maximum magnitude earthquakes are incorporated in the CEUS SSC model as summarized in Sections 2.5.2.2 and 2.5.2.3. This zone is currently recognized as comprising a portion of the PEZ (Reference 2.5-223).

3. **Selected Seismogenic and Capable Tectonic Sources Beyond the Site Region**

The fifth paragraph under **Eastern Tennessee Seismic Zone** of Item 3 under Item d of this SSAR section is replaced as follows.

NAPS ESP VAR 2.0-4

Using three different methods specific to the Eastern Tennessee seismic source, Bollinger (SSAR Reference 79) estimated an M_{max} of m_b 6.45. Chapman and Krimgold (SSAR Reference 57) used an M_{max} of m_b 7.25 for the Eastern Tennessee zone and for most other sources in their seismic hazard analysis of Virginia. Both of these more recent estimates of M_{max} are similar to the range of M_{max} values used in the 1986 EPRI studies. These estimates of maximum magnitude earthquakes are incorporated in the CEUS SSC model as summarized in Sections 2.5.2.2.5.2 and 2.5.2.3.

The last sentence of the third paragraph under **Charleston Seismic Zone** of Item 3 under Item d of this SSAR section is replaced as follows.

NAPS ESP VAR 2.0-4

The Charleston Zone as defined by the CEUS SSC Project is characterized by evidence of RLMEs (Reference 2.5-223). The Charleston RLME is described in Sections 2.5.2.2.4.1 and 2.5.2.3.

A sentence is added to the end of the fourth paragraph under **Charleston Seismic Zone** of Item 3 under Item d of this SSAR section as follows.

NAPS ESP VAR 2.0-4

These estimates of maximum magnitude earthquakes and recurrence rates are incorporated in the CEUS SSC model as summarized in Section 2.5.2.2.4.1. The Charleston RLME is discussed in Section 2.5.2.3.

NAPS ESP VAR 2.0-4

The last paragraph under **Charleston Seismic Zone** of Item 3 under Item d of this SSAR section is deleted.

The first paragraph under **New Madrid Seismic Zone** of Item 3 under Item d of this SSAR section is replaced as follows.

NAPS ESP VAR 2.0-4

The New Madrid Seismic Zone extends from southeastern Missouri to southwestern Tennessee and is over 620 miles west of the Unit 3 site. The New Madrid Seismic Zone is one of four RLME sources that comprise the Reelfoot Rift Zone as defined by the CEUS SSC (Figure 2.5.1-202) (Reference 2.5-223) and is defined by post-Eocene to Quaternary faulting and historical seismicity.

The last sentence of the sixth paragraph under **New Madrid Seismic Zone** of Item 3 under Item d of this SSAR section is replaced as follows.

NAPS ESP VAR 2.0-4

These estimates of maximum magnitude earthquakes and recurrence rates are incorporated in the CEUS SSC model as summarized in Section 2.5.2.2.4.2. The New Madrid Fault system RLME is discussed in Section 2.5.2.3.

NAPS ESP VAR 2.0-4

The last paragraph under **New Madrid Seismic Zone** of Item 3 under Item d of this SSAR section is deleted.

NAPS ESP VAR 2.0-4

2.5.1.1.6 Geologic Bases for Defining Relevant Source Zones

As stated above, the Unit 3 site is located within the ECC-AM seismotectonic source zone (Figure 2.5.1-202) (Reference 2.5-223). This zone is defined to include the region characterized by the presence of rifted and extended continental crust that developed as a result of Mesozoic rifting that resulted in the formation of the Atlantic Ocean. A tectonic feature of the Mesozoic extended crust within the ECC-AM is an older east-dipping basal detachment fault (decollement) that separates overthrusted Appalachian terranes from underlying Precambrian rocks of the North American craton (Section 2.5.1.1.4.c.1, SSAR Figures 2.5-2 and 2.5-8, and Reference 2.5-223). The tectonic evolution of the site region is summarized in SSAR Section 2.5.1.1.2 and Section 2.5.1.1.4.a. Seismicity within the ECC-AM is discussed in Sections 2.5.2.2.3.1 and 2.5.2.3. Johnson et al. (SSAR Reference 195) present a global study of earthquakes in stable continental regions (SCRs). This study and the update in the CEUS SSC (Reference 2.5-223) document the assessments that Mesozoic and younger extended crust has produced all **M** ≥ 7 stable craton earthquakes worldwide.

The PEZ is the seismotectonic zone located immediately west of the ECC-AM (Figure 2.5.1-202) (Reference 2.5-223). The definition of this zone is also based on the studies documented in SSAR Reference 195 and updates documented in Reference 2.5-223 that late Precambrian to early Paleozoic rifting (Iapetan crustal extension) formed zones of crustal weakness that exhibit a higher rate of seismic activity. The Iapetan rifted margin defined in SSAR Reference 49 includes that part of the continental crust that includes known or inferred normal faults that formed parallel to the passive margin of Laurentia during the late Proterozoic to early Paleozoic opening of the Iapetus Ocean (Reference 2.5-223). These faults occur in the older crust beneath the Appalachian decollement and appear to be the structures along which earthquakes in the Giles County zone (Section 2.5.1.1.4.d.2) and East Tennessee zone (Section 2.5.1.1.4.d.3) occur. Figure 2.5.1-202 shows the PEZ Wide (PEZ-W). This is an alternative geometry of the PEZ that is extended to the west to incorporate additional Iapetan-rifted crust. The western boundary of the PEZ-W follows the Rome trough in Kentucky and West Virginia, following the Kentucky River fault system (Reference 2.5-223). Seismicity within the PEZ is discussed in Sections 2.5.2.2.3.3 and 2.5.2.3.

The AHEX seismotectonic zone represents the region of highly extended crust that is the transition between the extended, thick continental crust that underlies the ECC-AM and the thinner mafic oceanic crust of the Atlantic Ocean basin (Figure 2.5.1-202) (Reference 2.5-223). This zone is located entirely offshore and approximates the continental shelf from Nova Scotia to Georgia. The eastward thinning wedge of highly extended transitional crust forming the AHEX is significantly thinner than the extended continental crust of the ECC-AM. This zone is characterized by a greater amount of rifting that resulted in both a thinner crust and the introduction of basalts and mafic intrusions. The transition crust of the AHEX appears to correspond with the East Coast magnetic anomaly and is mainly defined on the basis of these geophysical data (Reference 2.5-223). Seismicity within the AHEX is discussed in Sections 2.5.2.2.3.2 and 2.5.2.3.

NAPS ESP VAR 2.0-4

2.5.1.1.7 Information on the Mineral Earthquake

a. **Seismicity**

The August 23, 2011 **M** 5.8 Mineral earthquake resulted from reverse faulting at a relatively shallow depth, approximately 4.7 mi (7.5 km), in central Virginia (Figure 2.5.1-201) (References 2.5-232, 2.5-235, and 2.5-237). More recent analyses indicate that the main shock hypocenter originated at 6.0 ± 3.1 km depth (Reference 2.5-268). Seismicity in this region is attributed to the CVSZ, a previously recognized zone of seismicity that has produced numerous historical small and moderate earthquakes (see Section 2.5.1.1.4.d.1). The largest earthquake prior to the Mineral earthquake occurred in 1875 and had an estimated magnitude of about **M** 4.8 based on felt reports and reported damage (Reference 2.5-244). The most recent damaging earthquake prior to the Mineral earthquake was a magnitude 4.5 on December 9, 2003 (Reference 2.5-244). Both of these prior earthquakes were located in Goochland County, VA, near the James River and south of the Mineral earthquake epicenter.

In order to best represent the approximate rupture plane or fault that produced the Mineral earthquake, the aftershock information from various authors and as provided on the VTSO website (Reference 2.5-242) were used to develop a representation of the

possible rupture plane and its up-dip projection to the surface. These findings are summarized as follows:

- "This cluster [of aftershock hypocenters] spans a lateral distance of ~10 km and is centered beneath Yancyville on the South Anna River. The best fit plane to this cluster, the Quail fault (QF) strikes N30°E and dips 46°SE" (Reference 2.5-232).
- "The early aftershocks define a plane striking N29°E and dipping 51 degrees to the southeast" (Reference 2.5-235).
- "Given the regional trend of the geology and aftershock distribution, we prefer a fault plane that has a strike of 28 degrees and a dip of 55 degrees based on the University of Saint Louis regional CMT solution" (Reference 2.5-240).
- The inferred plane dips down 46 degrees to the east-southeast (Reference 2.5-241).

The up-dip surface projection, as shown on Figure 2.5.1-203, approximates where the fault may intersect the ground surface. Constraining the approximate location of the Mineral earthquake rupture plane allows for comparisons with the surface geology and geomorphology to assess the potential for surface deformation from the 2011 Mineral event or any past surface ruptures preserved in the landscape. Figure 2.5.1-203 was created in the following manner:

- Hypocenters from Reference 2.5-242 were plotted (color-coded by depth) along with the surface-projected aftershocks. The aftershocks were projected up-dip to the surface along a plane oriented N29°E and dipping 51°SE. The surface-projected aftershocks represent a best estimate of where the fault rupture would intersect the ground surface.
- A best-fit line was drawn through the surface-projected aftershocks (shown as a dark red dashed line on Figure 2.5.1-203). The orientation and length of this up-dip surface projection line are N30°E and 6.2 mi (10 km), respectively.
- An estimate of the vertical surface projection of the rupture plane was developed using information from Horton et al. (Reference 2.5-232) and is shown as a red dashed rectangle on Figure 2.5.1-203. This plane is located approximately 0.62 mi (1 km) southeast of the up-dip surface projection line, consistent with an approximately 45° dip and an estimated 0.62 to 4.7 mi (1 to 7.5 km) depth (Reference 2.5-232).

The rectangle represents the approximate vertical projection of a rupture plane with a dip of 46 to 51° from an upper depth of about 0.62 mi (1 km) and a lower depth of about 4.7 mi (7.5 km).

This interpretation shown on Figure 2.5.1-203 depicts an area where any surface rupture would likely be located. The subtle differences in strike and dip estimated by the seismologists cited above are considered as inherent uncertainty in the aftershock location calculations. The representation of the up-dip surface projection line (red dashed line) and vertical surface projection rupture plane (red dashed rectangle) in Figure 2.5.1-203A are also reproduced in Figure 2.5.1-204, 2.5.1-205, and 2.5.1-206. Figures 2.5.1-203B and 2.5.1-203C show plan and cross-section views, respectively, of the vertically projected rupture plane to illustrate the eastward-dipping nature of the rupture plane defined by the aftershocks.

b. **Geologic Reconnaissance**

A geologic field reconnaissance was conducted between April 19-21, 2012 to evaluate and document whether the August 23, 2011 **M** 5.8 Mineral earthquake produced coseismic surface rupture or other visible forms of surface deformation. To aid in the geomorphic and geologic assessment of the Mineral earthquake study area, Light Detection And Ranging (lidar) data were acquired to produce high-resolution topographic images in the epicentral area (Figure 2.5.1-207). The lidar data were processed to produce a bare earth model, which eliminates above ground points such as the tree canopy. The lidar package included:

- Digital Elevation Model (DEM)
- Hillshade Map
- Slope Map
- Contour Map (1 ft contour interval), and
- Orthophotography

The field reconnaissance focused primarily on the areas of the up-dip surface projection line and the vertical surface projection of the rupture plane (Figure 2.5.1-204). Several other areas that were also evaluated included the epicentral area along Shannon Hill Road, reported damage in the towns of Louisa and Mineral, road crossings of mapped faults, and the area immediately west of the North Anna site (Figure 2.5.1-204).

The up-dip surface projection line of the rupture plane is estimated to have an orientation of N30°E, dipping 45-50°SE and projects to the surface with a length of approximately 6.2 mi (10 km) between the town of Quail, VA to the southwest and the headwaters of Despar Creek to the northeast (Figure 2.5.1-204). This up-dip surface projection line is located entirely within the Chopawamsic Formation and Mine Run Complex (SSAR References 66 and 105) and is shown to cross the Chopawamsic fault (Figures 2.5.1-205 and 2.5.1-206) (References 2.5-241, 2.5-245, and SSAR Reference 66). Recent geological mapping (Reference 2.5-246), however, does not show the Mine Run Complex east of the Ellisville pluton nor the Chopawamsic fault, which would indicate that the up-dip surface projection line would be located entirely within the Chopawamsic Formation near the contact area with the Ellisville pluton (Section 2.5.1.2.3.f).

The study area (area of field reconnaissance) was evaluated for evidence of recent surface faulting from the 2011 Mineral earthquake, as well as evidence of repeated surface faulting. Subtle geomorphic evidence in the landscape may indicate where repeated surface or blind faulting may have occurred.

Evidence for potential surface faulting or deformation varies based on the perspective or scale of observations as well as the age and recurrence of potential past events. Prior to and following completion of the field reconnaissance, information in the lidar data collected for this study and derivative products were evaluated for evidence of regional fault-related geomorphic features, including geomorphic lineaments caused by active faulting, stream gradient changes or offsets, and contrasting large topographic features. Some of these evaluations are further discussed below.

The geologic field reconnaissance evaluated local geomorphic and anthropogenic features for more direct evidence of surface rupture associated with the Mineral earthquake. Based on the lack of field evidence immediately following the Mineral earthquake, the size of the postulated rupture plane, and the moderate magnitude of the earthquake, significant evidence for surface rupture was not anticipated and therefore efforts were focused on detecting other possible minor surface effects. Additionally, given the lack of numerous outcrops and exposures in the area, the field reconnaissance primarily focused on searching for evidence of recent rupture and deformation of roads and roadway

corridors, and confirming previously mapped geologic units as well as obtaining familiarity with the regional geology and geomorphology to better aid in interpretation of the lidar data.

Figure 2.5.1-204 shows the routes and waypoints of the field reconnaissance and the numerous roads that cross the projected surface trace of the rupture surface at oblique to near orthogonal angles. The pavement on these roads was in good condition and showed minimal distress cracking from age or settlement, making them excellent strain markers. No deformation in paved road surfaces was detected during the survey.

Within more active fault zones, geomorphic features may be found that have their origin in ground surface displacement and movement of fault-bounded slices within the fault zone. Transects of the study area specifically looked for field evidence of surface rupture that included the following:

- Ground fissures or compressional ground buckling;
- Springs or artesian conditions;
- Changes in vegetation growth;
- Minor fault scarps;
- Fault controlled drainages; and
- Cracked or offset pavement along roads.

None of these potential fault features were observed during the field reconnaissance. In addition, the reconnaissance effort did not observe any liquefaction features generated by the Mineral earthquake, as described in References 2.5-229 and 2.5-238, and summarized in Section 2.5.1.1.4.d.

The geomorphology of the study area is primarily controlled by the northeast strike of regional geologic structures. The structural grain is clearly reflected in the topography of the region as long, linear ridges and valleys such as those extending southwest from Lake Anna (Figures 2.5.1-205 and 2.5.1-207). In map view, the full length of many tributary streams follow regional structural grain, and nearly all streams exhibit local reaches that appear to be strongly influenced by underlying bedrock structure. At smaller scales, strong topographic lineaments such as those in the southwest corner of the study area are related to erodibility contrasts between and within geologic units.

c. **Conclusions**

- Geologic field reconnaissance and geomorphic assessment of the lidar data indicate that seismologic data, as opposed to geologic data, provide the best definition of the causative fault plane associated with the Mineral earthquake. As a result, aftershocks and focal mechanism solutions for the Mineral earthquake define a rupture plane striking approximately N30°E, and dipping 45-50°SE (Figure 2.5.1-204). Horton et al. (Reference 2.5-232) describe the rupture surface as an approximately 6.2 mi (10 km) long plane oriented N30°E, 46°SE that extends from about 4.7 mi (7.5 km) to 0.62 mi (1 km) in depth. Chapman (Reference 2.5-235) determined the rupture plane to be N29°E, 51°SE from early aftershocks in the sequence. Based on the field reconnaissance performed between April 19-21, 2012 no evidence of surface rupture, surface fault features, or geomorphic expression of surface rupture or coseismic surface tectonic deformation exists for the Mineral earthquake. Reconnaissance performed by the USGS, the Virginia Division of Geology and Natural Resources, researchers from Virginia Polytechnic Institute and State University, North Carolina State, and other academic institutions immediately following the earthquake concluded that the **M** 5.8 earthquake did not produce any discernible rupture or deformation at the ground surface.
- The Mineral earthquake does not appear to have occurred on a previously mapped fault. The surface projection of fault rupture crosses the trace of the Chopawamsic thrust and is near to the southeast margin of the Ellisville pluton tail. The Chopawamsic fault was reinterpreted as being truncated where it intersects the Ellisville pluton (Reference 2.5-246), making the sub-parallel contact between the Chopawamsic Formation and the Ellisville pluton the nearest mapped structural surface on which a fault could be located. It has been suggested that this contact is faulted, based on offset dikes mapped in the region, and is a possible candidate for the causative fault for the Mineral earthquake.
- The mainshock and deep aftershock epicenters are located near the mapped Long Branch fault. However, the up-dip projection of the aftershock rupture plane places the surface rupture several miles west of the Long Branch fault.

2.5.1.2.3 Site Area Stratigraphy

The third paragraph of this SSAR section is supplemented as follows with information that addresses the geological and geotechnical data collected from the additional Unit 3 borings.

NAPS COL 2.0-26-A

Seven borings were completed to depths ranging between 15 and 52 m (50 and 170 ft) during the ESP investigation (SSAR Appendix 2.5.4B). To supplement the existing geological and geotechnical data, 93 borings, 23 cone penetrometer tests (CPTs), 6 test pits, 5 sets of borehole geophysical logging, 5 sets of shear wave suspension logging, and 2 sets of electrical resistivity tests were performed as part of the subsurface investigation program for Unit 3. The boring data and geotechnical testing are discussed in detail in Section 2.5.4. The data developed by the Unit 3 subsurface investigation program are presented in Appendices 2.5.4AA, 2.5.4BB, and 2.5.4CC.

b. Ta River Metamorphic Suite (Cambrian and/or Ordovician)

The fourth paragraph of Item b of this SSAR section is supplemented as follows with information that summarizes the Unit 3 subsurface investigation program.

Borings completed during previous subsurface investigations at the NAPS site (SSAR References 7 and 8; and SSAR Appendix 2.5.4B) and borings completed as part of the Unit 3 subsurface investigation encountered rocks of the Ta River Metamorphic Suite at the Unit 3 site. (Appendices 2.5.4AA, 2.5.4BB, and 2.5.4CC)

Paragraphs six through ten of Item b of this SSAR section are supplemented as follows with information describing the results of the subsurface investigation performed for Unit 3.

NAPS ESP COL 2.5-1

Borings completed at the Unit 3 site as part of the Unit 3 subsurface investigation, documented in SSAR Reference 7, SSAR Appendix 2.5.4B, Appendices 2.5.4AA, 2.5.4BB, and 2.5.4CC, encountered the top of the moderately to highly weathered rock (Zone III) from about Elevation 206 to 292 ft. The maximum thickness of the Zone III rock measured about 23.47 m (77 ft) and is described in the boring logs as a yellowish brown, gray, tan, reddish brown and dark green, very severely to moderately weathered, very closely to closely fractured, very soft to hard, biotite quartz gneiss and quartz biotite gneiss,

with traces of clay, iron oxide staining, magnetite, muscovite and feldspar. In the central portion of the power block area, the Zone III rock is typically between elevations of about 260 to 280 ft. To true north and true south, this rock is typically at elevations of less than 240 ft. In three of the borings (M-11, B-917, and B-913) the top of the Zone III rock is at an elevation less than 220 ft. Of the three borings, the lowest recorded top of Zone III rock elevation is in boring B-917 at about 207 ft. The thickness of the saprolite overlying the Zone III rock is typically greatest at these boring locations, and in boring M-11 the combined thickness of Zones IIA and IIB saprolite reaches a maximum thickness of about 114 ft. The top of the slightly weathered to moderately weathered rock (Zone III-IV) was encountered in the borings at elevations ranging from about 187 to 292 feet and is generally described in the boring logs as a reddish brown to gray, moderately to slightly weathered, very close to moderately fractured, soft to very hard, biotite quartz gneiss and quartz biotite gneiss. The top of the slightly weathered to fresh rock (Zone IV) was encountered in the borings at elevations ranging between about 171 and 278 feet and is generally described in the boring logs as a gray and reddish brown, slightly weathered to fresh, very close to widely fractured, very hard, biotite quartz gneiss and quartz biotite gneiss. In the central portion of the power block area the top of Zone III-IV rock is typically between elevations of about 240 ft to 270 ft, with the exception of three borings (B-901, W-1, and B-903) where the top of Zone III-IV rock is at elevations of approximately 229 ft, 211 ft and 221 ft, respectively. To true north and true south, the top of the Zone III-IV rock is typically at an elevation less than 220 ft and a number of the borings exhibited an elevation less than 210 ft. The lowest recorded top of Zone III-IV rock elevation is in borings B-917 and W-9 at approximately 187 ft.

The last paragraph of Item b of this SSAR section is supplemented with a new paragraph on Unit 3-specific geologic boring results.

The borings exhibit severely weathered and jointed intervals in the Zone III-IV and Zone IV rock. These intervals were encountered in several of the borings at varying elevations ranging from 150 ft to 285 ft. The intervals ranged in thickness from 0.2 to 20 ft (Appendices 2.5.4AA, 2.5.4BB, and 2.5.4CC). Characteristically, these intervals comprise poor to very poor quality rock that is highly fractured or jointed. The joints (typically sets of 3 to 10 joints) exhibit clay filling, iron and manganese

oxide staining and occasionally quartz and feldspar veins. Occasionally, water loss in the fracture zones is reported to have occurred during drilling. In boring W-1 a micro-shear zone in the Zone III-IV rock was encountered at an elevation of about 210 ft. It is described in the boring log as a possible shear zone, 0.6 ft thick comprising soft, yellow-brown clay with rock fragments. Quartz and feldspar veins encountered in the Zones III-IV and IV rock commonly contain traces of mica, garnet, magnetite, calcite, pyrite and occasional chlorite and epidote. These veins range in thickness from less than 0.1 ft to 0.8 ft. The thickest quartz vein at 0.8 ft thick encountered in boring M-1 is at an elevation of approximately 123 ft.

f. **Ellisville Pluton (Silurian)**

A new paragraph is added after the last paragraph of Item f of this SSAR section as follows.

Recent geologic mapping at a scale of 1:24,000 in the northern half of the Ferncliff, VA 7.5' quadrangle indicates that the Ellisville pluton appears to cross-cut and post-date the Chopawamsic thrust fault. This geologic mapping and age dating presented by Hughes and Hibbard (Reference 2.5-246) indicate that the Ellisville pluton (approximately 440 million years old) postdates thrusting and sinistral motion on the Chopawamsic fault (Section 2.5.3.2.1). It has been suggested that the contact between the Ellisville pluton and the Chopawamsic Formation, which is sub-parallel to the Chopawamsic fault, is faulted. Although this new interpretation by Hughes and Hibbard (Reference 2.5-246) makes the contact between the Chopawamsic Formation and the Ellisville pluton the nearest mapped structural surface on which the Mineral Earthquake might have occurred, the geologic reconnaissance described in Section 2.5.1.1.7 found no evidence for surface faulting.

h. **Residual Soil and Saprolite (Cenozoic)**
Residual Soil

The second paragraph of Item h of this SSAR section is supplemented as follows with information to address residual soil characterization.

Residual soil was not encountered in any of the borings drilled as part of the Unit 3 subsurface investigation. (Appendices 2.5.4AA, 2.5.4BB, and 2.5.4CC)

Saprolite

Paragraph five of Item h of this SSAR section is supplemented as follows with a new paragraph that addresses geologic findings relative to saprolite.

Borings drilled as part of the subsurface investigation for Unit 3 encountered the top of the Zone IIA saprolite at elevations ranging from about 232 to 335 ft. The thickest Zone IIA saprolite encountered was about 28.65 m (94 ft) while the median thickness was about 9.14 m (30 ft). The saprolite is generally described in the boring logs as a yellowish red to yellowish brown to pale brown to greenish brown, medium dense to dense, clayey silt, silty sand and sand with relict rock fabric. The top of the Zone IIB saprolite was encountered at elevations ranging from about 215 to 302 ft. The thickest Zone IIB saprolite encountered was about 13.1 m (43 ft) while the median thickness was about 2.44 m (8 ft). The saprolite is generally described in the boring logs as a pale brown to reddish and yellowish brown to brownish gray to greenish gray, very dense, fine to coarse grained sand and very severely weathered, soft to moderately hard gneiss with traces of clay, mafic minerals, and iron oxide staining.

k. **Artificial Material**

The first paragraph of Item k of this SSAR section is supplemented as follows with information to address findings relative to artificial material.

Borings performed as part of the subsurface investigation for Unit 3 encountered fill to depths of between about 0.12 to 5.48 m (0.4 and 18 ft) below the ground surface. The maximum thickness of fill (18 ft) was encountered in boring B-932 and is described in the boring log as a greenish gray and yellowish brown sandy silt and clay with traces of gravel and organic debris. Asphalt and road base, typically less than about one foot thick, was encountered in a number of borings (Appendices 2.5.4AA, 2.5.4BB, and 2.5.4CC).

The first paragraph of Item k of this SSAR section is supplemented with information on prohibiting the use of Zone IIA soil as structural fill.

NAPS ESP PC 3.E(5)

As described in Section 2.5.4.5.3, Zone IIA soil will not be used as structural fill to support Seismic Category I or II structures.

2.5.1.2.4 Site Area Structural Geology

The second sentence of the third paragraph of this SSAR section is replaced as follows.

NAPS ESP VAR 2.0-4

None of these faults are considered capable tectonic sources, as defined in RG 1.208, Appendix A.

2.5.1.2.6 Site Engineering Geology Evaluation

a. Engineering Behavior of Soil and Rock

Soil

The second paragraph under Soil in Item a of this SSAR section is supplemented as follows with information to address soil behavior.

NAPS COL 2.0-26-A

The saprolite at the Unit 3 site has been categorized into Zone IIA and Zone IIB saprolite, based on its general composition and grain size (Section 2.5.4). Grain size tests on samples of the Zone IIA saprolite show that the median fines content for the saprolite is about 24 percent with the majority of the samples classified as a silty sand (SM). Grain size tests on samples of the Zone IIB saprolite show that the fines content for the saprolite ranges from about 15 to 27 percent. The saprolite is also classified as a silty sand (SM). Zone IIA saprolite is the more weathered of the two saprolites and contains less than 10 percent rock fragments with relict texture. The borings drilled as part of the subsurface investigation for Unit 3, documented in Appendices 2.5.4AA, 2.5.4BB, and 2.5.4CC, reveal that SPT N-values ranged from 2 to refusal, with a median value of 15 blows per foot (bpf) for this saprolite. Zone IIB saprolite contains between 10 and 50 percent relict rock fragments, and SPT N-values ranged from 24 to refusal with a median value of 75 bpf. Section 2.5.4 contains a detailed discussion of the geotechnical properties of the saprolite at the Unit 3 site.

Rock

The second paragraph under Rock of Item a of this SSAR section is supplemented as follows with information to address rock behavior.

Based on the results of the borings drilled as part of the subsurface investigation for Unit 3, documented in Appendix 2.5.4AA, rock quality designation (RQD) generally ranges from zero to 50 percent for the

Zone III rock with an average RQD value of about 20 percent. An RQD of 20 percent is indicative of very poor quality rock (SSAR Reference 109).

The third paragraph under Rock of Item a of this SSAR section is supplemented as follows with information to address rock behavior.

Based on the results of the borings drilled as part of the subsurface investigation for Unit 3 and documented in Appendices 2.5.4AA, 2.5.4BB, and 2.5.4CC, RQD generally ranges from about 50 to 90 percent for the Zone III-IV rock with an average value of about 65 percent, indicative of fair quality rock (SSAR Reference 109). For the Zone IV rock, RQD is generally above 80 percent and mostly above 90 percent. The average RQD value is 95 percent, indicative of excellent quality rock (SSAR Reference 109). The boring results for the previous geotechnical investigations (SSAR References 7 and 8), and for both the ESP subsurface investigation (Reference 2.5-201) and the Unit 3 subsurface investigation (Appendices 2.5.4AA, 2.5.4BB, and 2.5.4CC) indicate that Zones III, III-IV and IV are suitable bearing surfaces on which to found the Seismic Category I structures. The RB, Fuel Building, and the Control Building, will be founded on the Zone III-IV or Zone IV bedrock; where the top of this bedrock is below the foundation level, the overlying materials will be replaced with concrete fill. The FWSC will be founded on Zone III rock or on concrete fill above the top of the Zone III rock. The joints and fractures present in these zones are not of sufficient density or areal extent to affect the engineering behavior of the rock with respect to its foundation bearing capacity or integrity.

b. **Zones of Alteration, Weathering and Structural Weakness**

The third paragraph of Item b of this SSAR section is supplemented as follows with information to address zones of alteration, weathering and structural weakness.

Borings completed as part of the ESP subsurface investigation program (SSAR Appendix 2.5.4B) and the Unit 3 COL subsurface investigation programs (Appendices 2.5.4AA, 2.5.4BB, and 2.5.4CC) reveal zones of severely weathered and fractured rock in the moderately to slightly weathered (Zone III-IV) and slightly weathered to fresh rock (Zone IV). The zones are at elevations ranging between about 150 ft and 285 ft and range in thickness from 0.2 ft to 20 ft with a median thickness of about

5 ft. RQD values in these zones range from 0 to 40 percent with a median value of about 10 percent. Characteristically, these fracture zones exhibit clay filling, iron and manganese oxide staining and, occasionally, quartz and feldspar veins. Occasionally, water loss in the fracture zones is reported to have occurred during drilling.

The fourth paragraph of Item b of this SSAR section is supplemented as follows with information on excavation and replacement of weathered or fractured rock.

NAPS ESP PC 3.E(4)

Weathered or fractured rock at the foundation level for safety-related structures will be excavated and replaced with lean concrete before initiation of foundation construction. See also Section 2.5.4.10.

d. Prior Earthquake Effects

The last sentence of the second paragraph of Item d of this SSAR section is replaced as follows.

NAPS ESP VAR 2.0-4

The Unit 3 site is located within the CVSZ, which is an area of persistent, low-level seismicity in the Piedmont Province and ECC-AM source zone, as described in Section 2.5.1.1.4.d.1. (Reference 2.5-223)

f. Construction Groundwater Control

The first paragraph of Item f of this SSAR section is supplemented as follows with information to address ground water level.

Groundwater levels at the site are expected to result in the need for temporary dewatering of foundation excavations extending below the water table. Dewatering will be performed in a manner that minimizes drawdown effects on the surrounding environment. Drawdown effects will be limited to the Unit 3 site and no offsite users will be affected.

g. Unforeseen Geologic Features

The first paragraph of Item g of this SSAR section is supplemented as follows with information to address geologic mapping of excavations of safety-related structures.

NAPS ESP PC 3.E(6)

Future excavations for safety-related structures will be geologically mapped. Unforeseen geologic features that are encountered will be

evaluated. The NRC will be notified no later than 30 days before any excavations for safety-related structures are open for NRC examination and evaluation. See also Section 2.5.4.5.2.

2.5.1.2.7 Site Groundwater Conditions

The second paragraph of this SSAR section is supplemented as follows with information to address site groundwater conditions.

NAPS COL 2.0-26-A

A detailed discussion of Unit 3 site groundwater conditions based on the Unit 3 subsurface investigation is provided in Section 2.4.12.

NAPS COL 2.0-26-A **Figure 2.5.1-201 Lidar Survey Location Map**

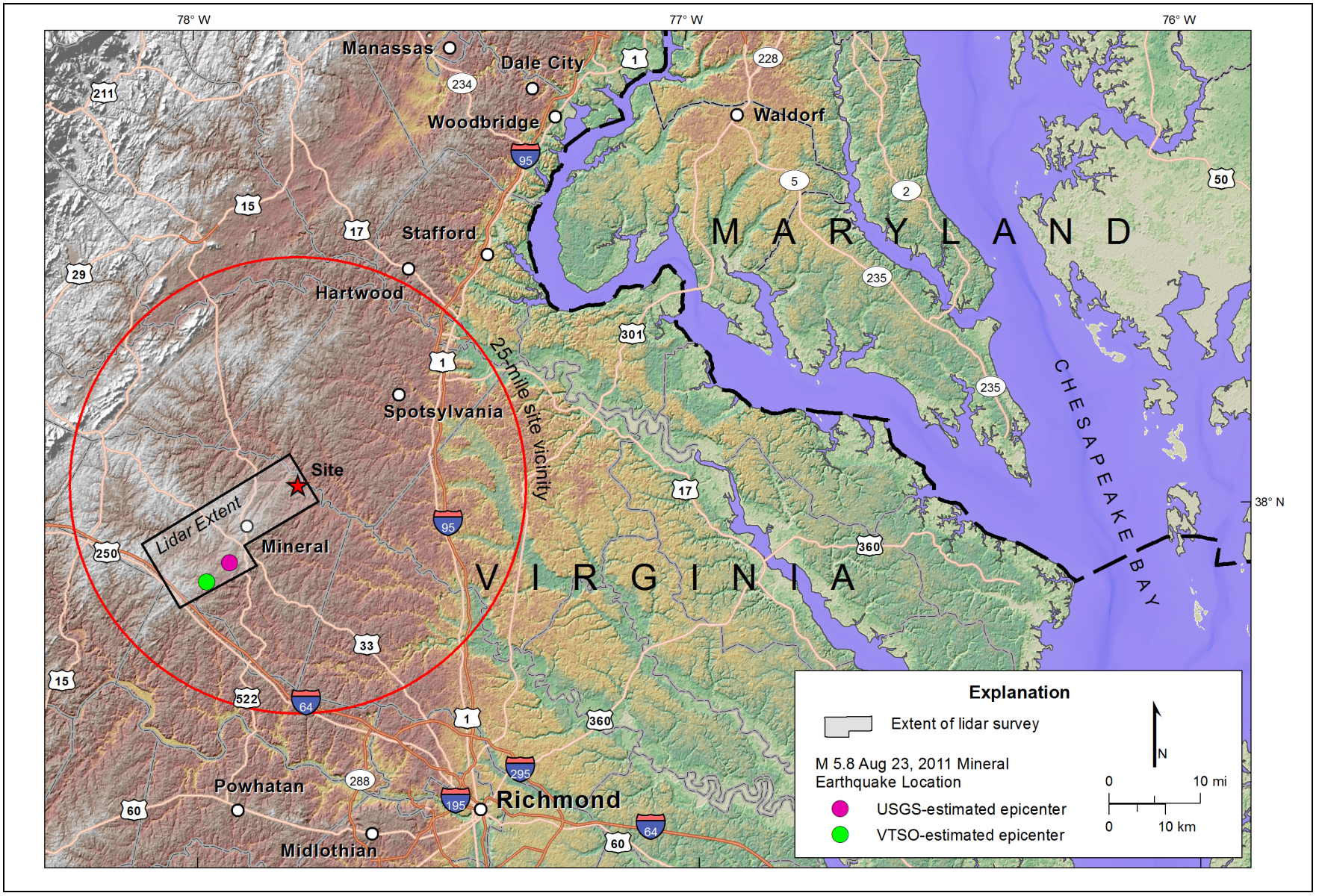

BASIS: ESBWR COLA

NAPS COL 2.0-26-A **Figure 2.5.1-202 CEUS SSC Sources Zones**

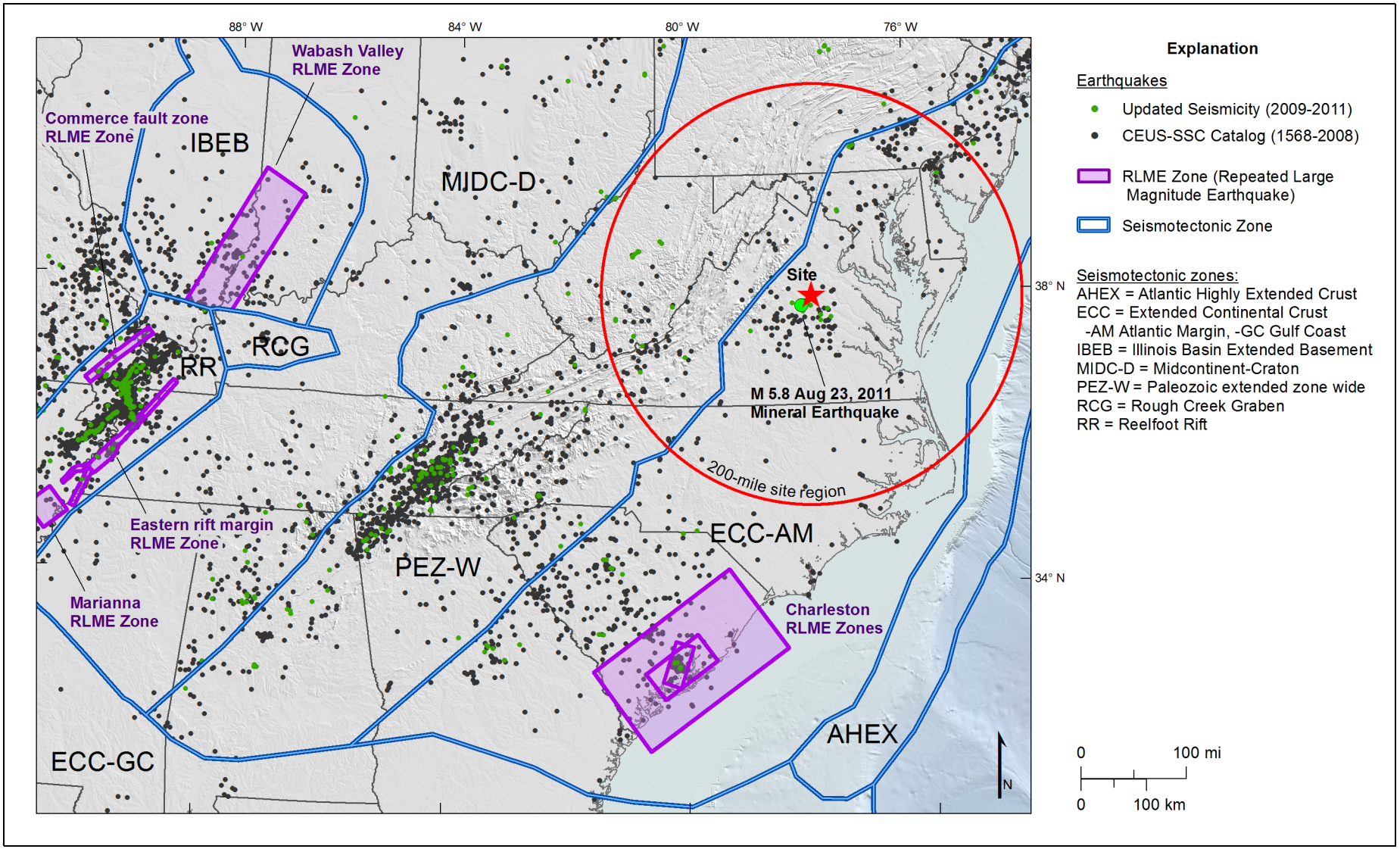

NAPS COL 2.0-26-A **Figure 2.5.1-203(A), (B), and (C) Mineral Earthquake Hypocentral Data**

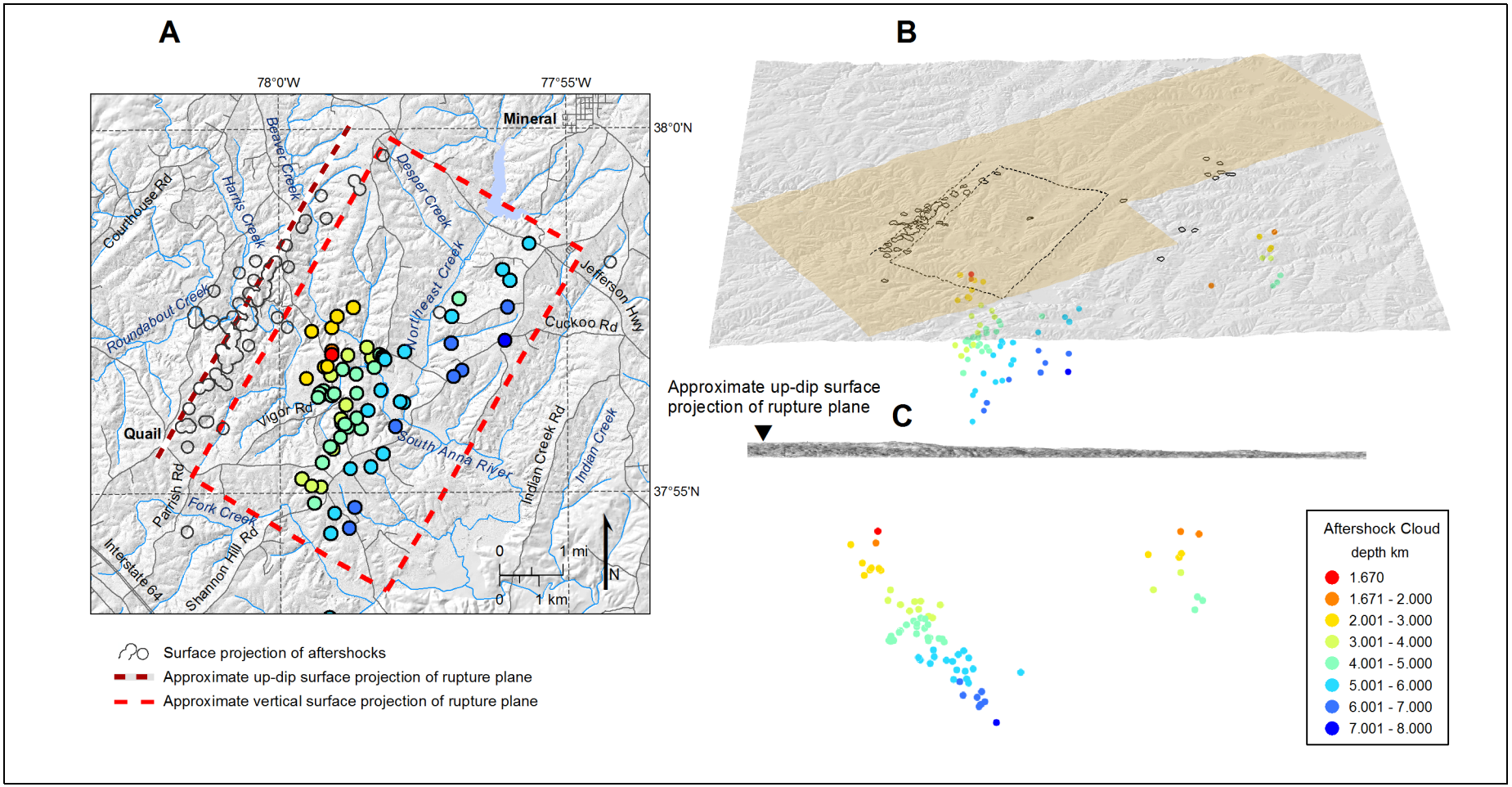

Notes:

1. Map of approximate vertical projection (dashed rectangle) of rupture plane estimated from August 25–September 1, 2011 aftershocks (Reference 2.5-242) and approximate up-dip surface projection of rupture plane (dashed line) based on surface projected aftershocks. These surface-projected aftershocks define the area where fault would intersect the ground surface.
2. 3-dimensional perspective view of aftershocks defining the rupture plane (view to the north).
3. Aftershocks defining eastward dip of fault (view N30E along strike of rupture).

NAPS COL 2.0-26-A **Figure 2.5.1-204 Field Reconnaissance Routes and Waypoints**

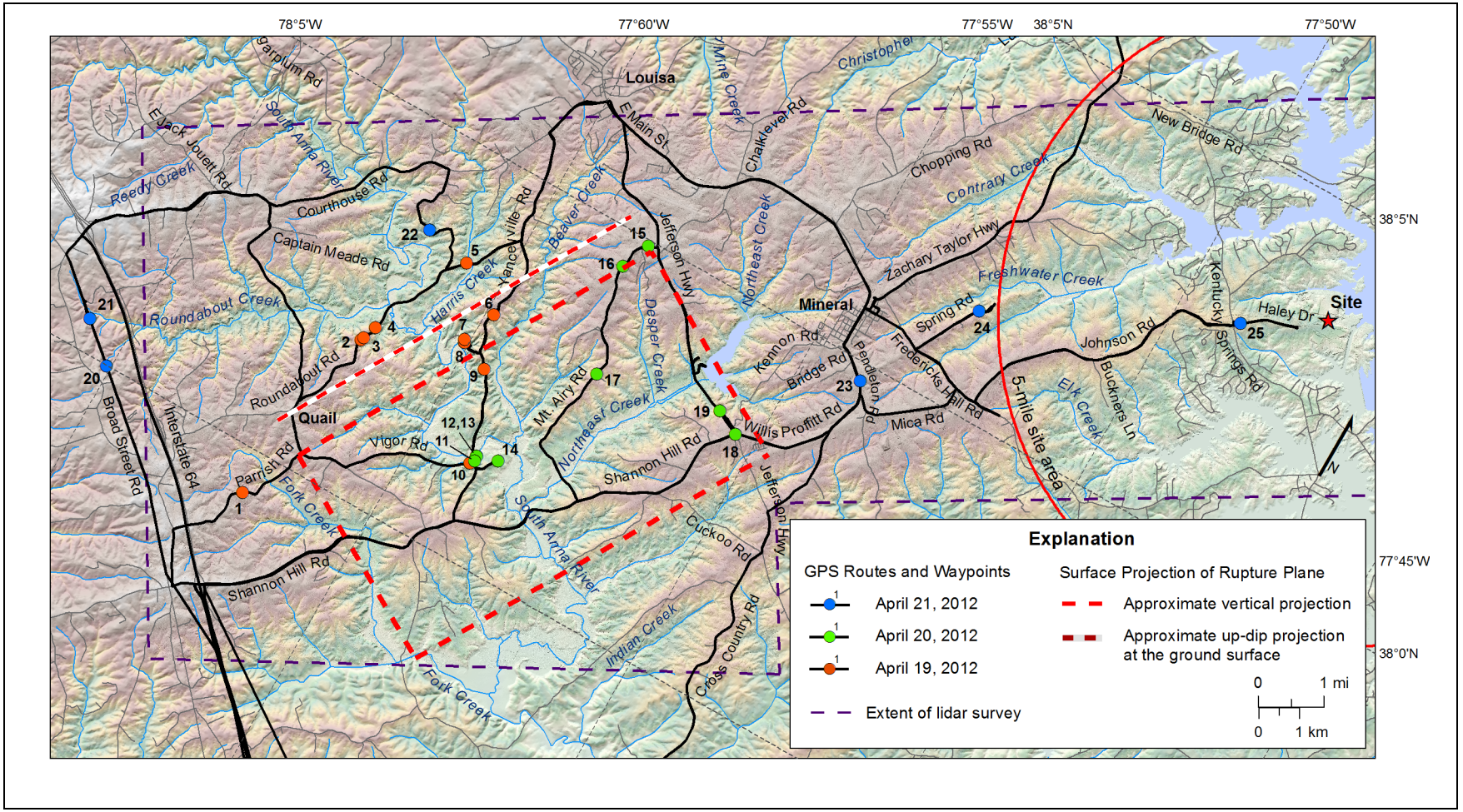

NAPS COL 2.0-26-A **Figure 2.5.1-205 Geologic Map of the Mineral Earthquake Study Area (1:500,000 scale)**

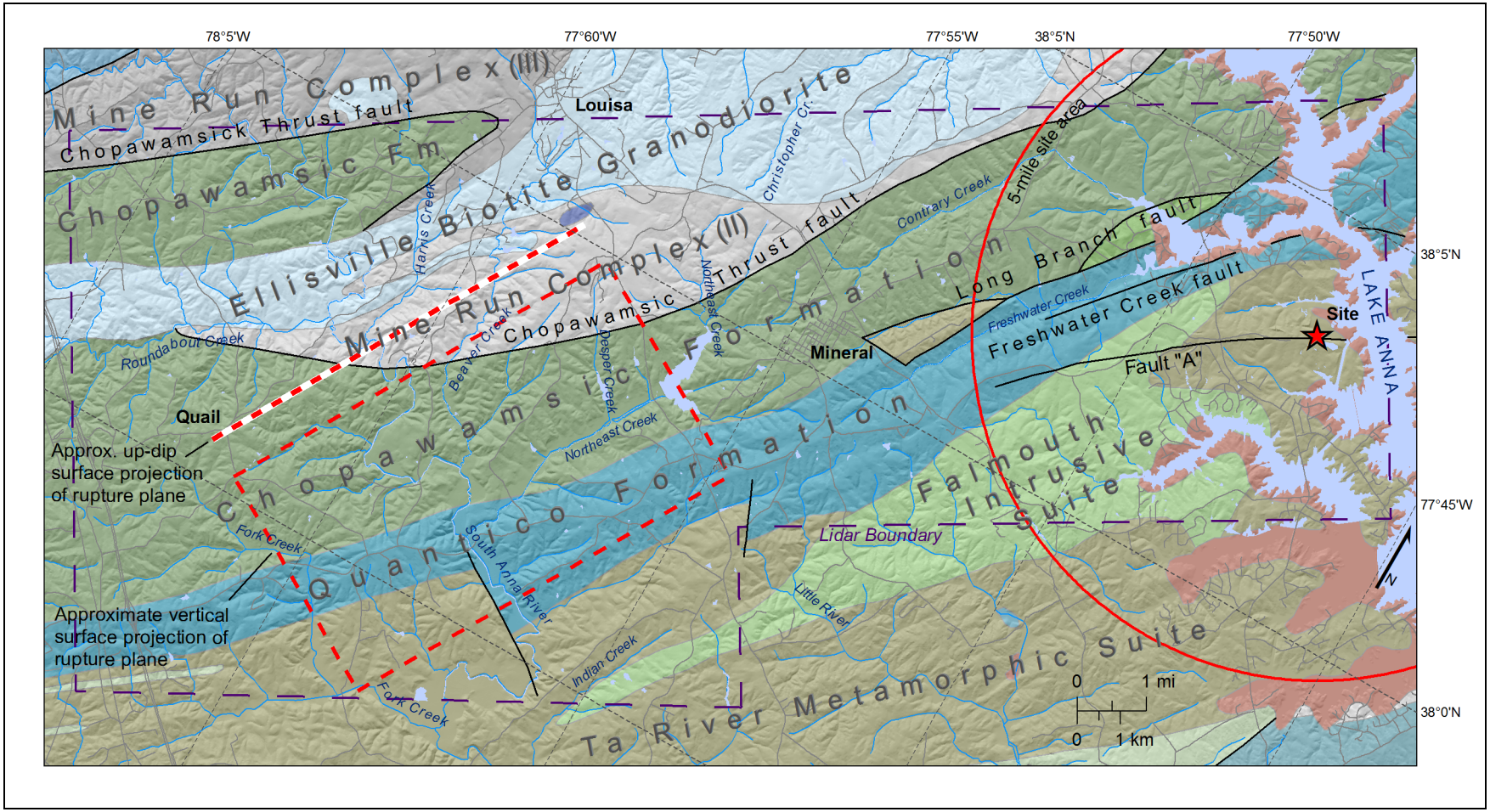

NAPS COL 2.0-26-A **Figure 2.5.1-206 Geologic Compilation Map with Numbered GPS Waypoint Locations**

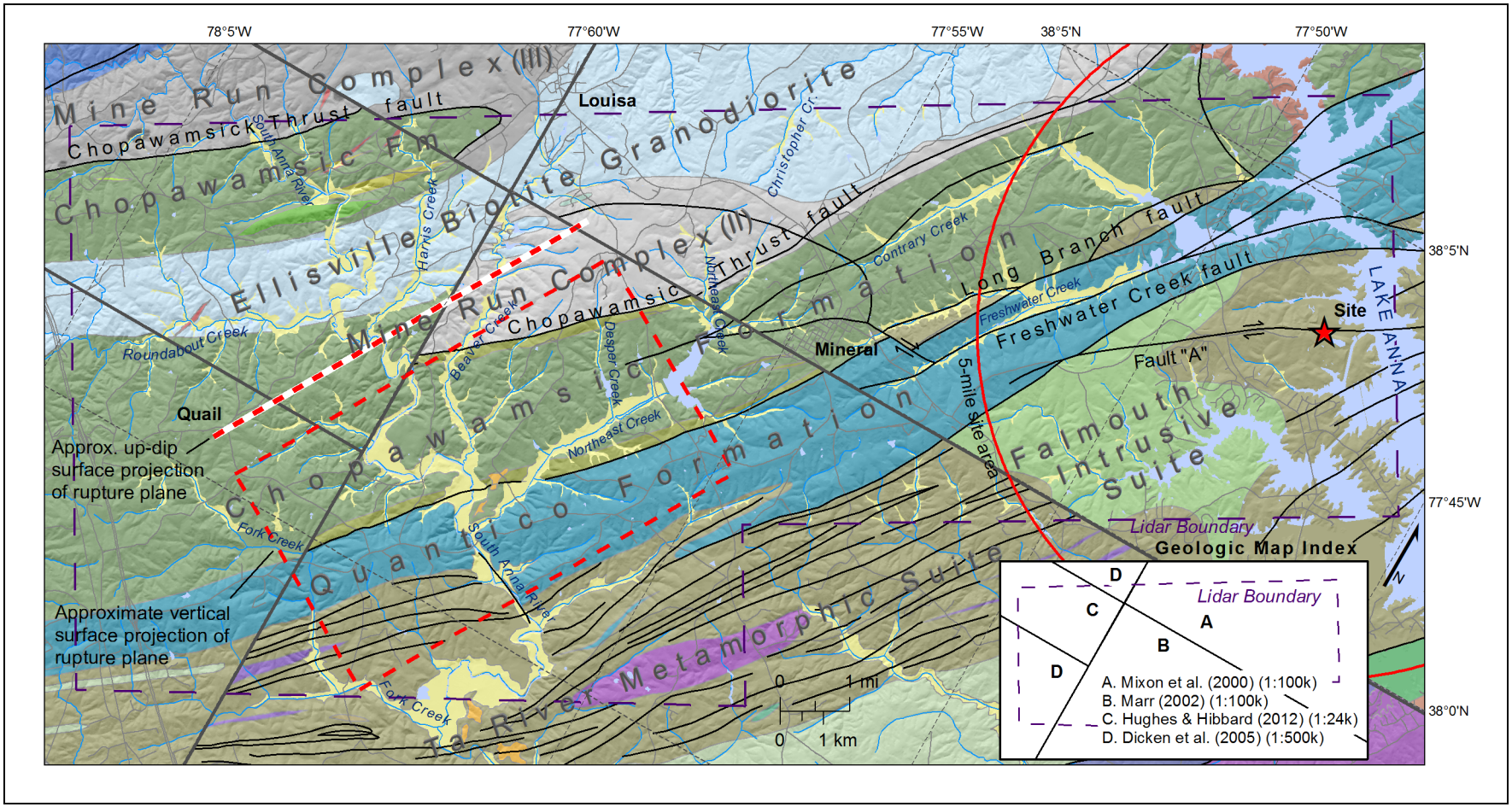

Notes:

1. Mismatches in geologic units at map boundaries.
2. Faults shown as thin black lines.
3. Low relief associated with Ellisville biotite granodiorite pluton.
4. Contact area is from 1:500,000-scale geologic map.

NAPS COL 2.0-26-A **Figure 2.5.1-207 Color-Shaded Relief Map**